10-14-2003

Auroral source region: Plasma properties of the high-latitude plasma sheet

C. A. Kletzing
University of Iowa

J. D. Scudder
University of Iowa

E. E. Dors
Los Alamos National Laboratory, Los Alamos, New Mexico

Carina Curto
University of Nebraska - Lincoln, ccurto2@math.unl.edu

Auroral source region: Plasma properties of the high-latitude plasma sheet

C. A. Kletzing and J. D. Scudder
Department of Physics and Astronomy, University of Iowa, Iowa City, Iowa, USA

E. E. Dors
Los Alamos National Laboratory, Los Alamos, New Mexico, USA

C. Curto
Department of Mathematics, Duke University, Durham, North Carolina, USA

Received 9 September 2002; revised 5 June 2003; accepted 20 June 2003; published 14 October 2003.

[1] Statistical results from a survey of 93 passes through the high-latitude extension of the plasma sheet of electron data from the Hydra instrument on the Polar spacecraft show that the values for electron density can range from 0.01 to 0.5 cm^{-3} with an average value around 0.1 cm^{-3} on the poleward side and 0.3 cm^{-3} on the equatorward side. Electron mean energy is found to have an average value near 900 eV on the equatorward side and 400 eV on the poleward side but varies from 100 eV to 4 keV. These values for density and mean energy are similar to those reported for measurements made in the equatorial plasma sheet by several previous spacecraft. The character of the electron distributions has been compared with Maxwellian and κ-distributions with the result that the κ-distribution with $\kappa \leq 10$ yields an acceptable fit to the data twice as often as a Maxwellian distribution. This is similar to results found in the equatorial plasma sheet for both electrons and ions. The variation of electron density and mean energy around their average values have been compared with several solar wind parameters which have been developed to correlate solar wind variation with magnetospheric activity level. Few of these parameters are found to provide significant correlation with high-latitude plasma sheet electron density or temperature with the notable exception of solar wind density and solar wind particle flux which correlate with plasma sheet density. *INDEX TERMS:* 2764 Magnetospheric Physics: Plasma sheet; 2736 Magnetospheric Physics: Magnetosphere/ionosphere interactions; 2704 Magnetospheric Physics: Auroral phenomena (2407); 2784 Magnetospheric Physics: Solar wind/magnetosphere interactions;
KEYWORDS: plasma sheet, aurora, temperature, density, solar wind correlation

Citation: Kletzing, C. A., J. D. Scudder, E. E. Dors, and C. Curto, Auroral source region: Plasma properties of the high-latitude plasma sheet, *J. Geophys. Res.*, *108*(A10), 1360, doi:10.1029/2002JA009678, 2003.

1. Introduction

[2] The Earth's plasma sheet is a unique interface between plasma processes in the the magnetotail and the ionosphere. The plasma properties of the equatorial plasma sheet have been studied most extensively for the ion population of the central plasma sheet [*Huang and Frank*, 1986; *Baumjohann et al.*, 1989; *Kistler et al.*, 1993; *Huang and Frank*, 1994; *Wing and Newell*, 1998]. This is largely due to the fact that for studies of pressure balance between the tail lobes and the equatorial plasma sheet, only 15% of the pressure is contributed by electrons [*Spence et al.*, 1989; *Baumjohann et al.*, 1989] Similarly, momentum transport by high-speed flows is also dominated by the ion contribution due to their much greater mass. The ion density in the central plasma sheet is of the order of 0.3 cm^{-3} and the ion temperatures range from 3 to 7 keV. The ions in the plasma sheet boundary layer have lower densities and temperatures than those of the central plasma sheet with average densities 0.1 cm^{-3} and average temperatures which are about half of those in the central plasma sheet [*Baumjohann et al.*, 1989].

[3] The plasma sheet electron population is important because its high-latitude extension provides the source particles for the auroral region. Previous studies of plasma sheet electrons have found that these electrons have the same density as the ions (as would be expected) and temperatures which are typically a factor of 5–7 lower than those of the electrons [*Slavin et al.*, 1985; *Baumjohann et al.*, 1989]. Both plasma sheet electrons and ions frequently exhibit non-Maxwellian character with distributions often better described by the κ-distribution [*Christon et al.*, 1988, 1989]. In addition, near-Earth electron observations show evidence of counterstreaming electron populations [*Frank et al.*, 1996]. This has been attributed to acceleration of these

0148-0227/03/2002JA009678$09.00

electrons by auroral processes [*Kletzing and Scudder*, 1999].

[4] This paper focuses on the properties of the electron populations of the high-latitude plasma sheet above the auroral zone as measured by transits of the Polar spacecraft through this region. Electron density and mean energy at the poleward and equatorward edges of the Polar passes are examined to determine average values which correspond to boundary and central plasma sheet electron populations. The character of the distributions is compared with Maxwellian and κ-distributions to determine which is, on average, a better description of the high-latitude plasma sheet electrons. Finally, we examine the correlation between the variation in density and mean energy of the high-latitude electrons with various solar wind parameters that have been used as predictors of magnetospheric activity.

2. Instrument and Measurements

[5] The Hydra instrument on the Polar spacecraft consists of two separate particle measurement systems, the DuoDeca Electron Ion Spectrometer (DDEIS) and the Parallel Plate Analyzer (PPA). The DDEIS measures electron and ion spectra in broad angular bins ($8° \times 8°$) at 12 look directions in 1.15 s energy sweeps from 12 eV to 18 keV. Alternate sweeps simultaneously measure all 12 directions for electrons and then ions, yielding a time resolution for either species of 2.3 s. As the spacecraft rotates, complete coverage of all pitch angles is obtained. For the bulk properties of the plasma sheet electrons, the DDEIS data is sufficient and the PPA data was not used. Complete details of the instrumentation can be found in the work of *Scudder et al.* [1995].

[6] We have surveyed 93 orbits of Hydra data from February–May of 1997 when Polar passed through the high-latitude plasma sheet. These orbits provide coverage of the evening auroral zone over an MLT range of 2000–0300 at distances of 4–7.5 R_E geocentric which are well above the auroral acceleration region. Of the 93 orbits surveyed, 37 provide crossings in the premidnight sector and 56 crossings in the postmidnight sector. These smaller number of premidnight passes arise from spacecraft operations in the month of May 1997 which eliminated several orbits from the study. The Polar orbit is such that it is always in this MLT region and altitude range at the same time of year. The electron properties presented are therefore limited to this season for these MLT values. This may introduce some bias to the data, but it is unavoidable. However, the period of study does not extend into summer when ionospheric conductivity effects become more important, so it is unlikely that the effect of season is large.

[7] For the portions of this study which focus on density and temperature moments of the measured electrons, we have discarded orbits for which the data may be questionable. This includes orbits during times when the PSI potential control device operated because this may affect the measurement of lower energy electrons. In addition, moment calculations can be inaccurate when the peak energy of the electrons is not within the measured energy range. Orbits for which the plasma sheet signature appeared to have significant fluxes above the highest measured energy are also not included. After these orbits were removed, 78 orbits remained. The magnetic activity for the remaining orbits was generally low. For the 3 hours preceding the pass and during the pass, 80% of the passes had $K_p \leq 2$; 9% had $2 < K_p < 3$; and 9% had $3 < K_p < 4$. Only one pass had $K_p > 4$, with a value $K_p = 5$.

3. Temperature and Density

[8] Figure 1 shows Hydra data for a Polar passage across the high latitude plasma sheet on 16 March 1997. As time increases, the spacecraft is moving equatorward (toward lower invariant latitude). The bottom two panels of Figure 1 which show energy-time spectrograms of the differential energy flux of ions (bottom panel) and electrons (one above bottom panel). The polar cap is clearly demarcated by the absence of ions (particularly those at higher energies) in the energy range of the Hydra sensors and only minimal flux of electrons below 1 keV. Polar encounters the poleward boundary of the high latitude plasma sheet at 1237 UT as indicated by the appearance of ions at energies above 1 keV and the appearance of electrons with energies of a few hundred eV and with energies above those of the background polar cap electron "drizzle" at energies at or below 200–300 eV. We identify the equatorward boundary of the plasma sheet as the location where the upper energy cutoff of the plasma sheet electrons falls to zero between 1330 and 1335. This is the same boundary as the "B1" boundary that has been used by *Newell et al.* [1996]. In the work that follows, this boundary will be used as the equatorward boundary of the high latitude plasma sheet and the last occurrence of plasma sheet ions (similar to the *Newell et al.* [1996] "B5" boundary) will be used as the poleward boundary.

[9] The top panel of Figure 1 shows the electron density calculated from a moment of the measured electrons. The panel below the the top panel shows the mean energy moment of the measured electrons. In Figure 1 and those which follow, the mean energy moment is given as the energy-equivalent temperature using the usual relation of $kT = 2\bar{E}/3$. Both panels show typical values and morphology. The poleward side of the high-latitude plasma sheet has a somewhat lower density than the equatorward side with an overall average value of 0.2 cm^{-3}. The mean energy varies from lower values near 400–500 eV up to a peak value of 2 keV. Note that the increase of the mean energy equatorward of the equatorward boundary of the high-latitude plasma sheet comes from the very low fluxes at the very highest energies measured by the Hydra analyzer.

[10] To characterize the properties and variations of the high-latitude plasma sheet, a 15 min average of the density and mean energy moments was computed near the poleward and equatorward boundaries of each of plasma sheet crossings discussed above. The average ensures that small-scale variations in the structure of the plasma sheet do not unduly influence the study of the background properties. For the poleward boundary, the average was computed so that it began at the poleward edge and proceeded for 15 min toward the equatorward direction. For the equatorward boundary, the average was placed somewhat before the zero-crossing boundary so that the very low energy electrons which mark this boundary did not unduly influence the parameters. The exact location was chosen so as to represent the average value of the density and mean energy of the high-latitude

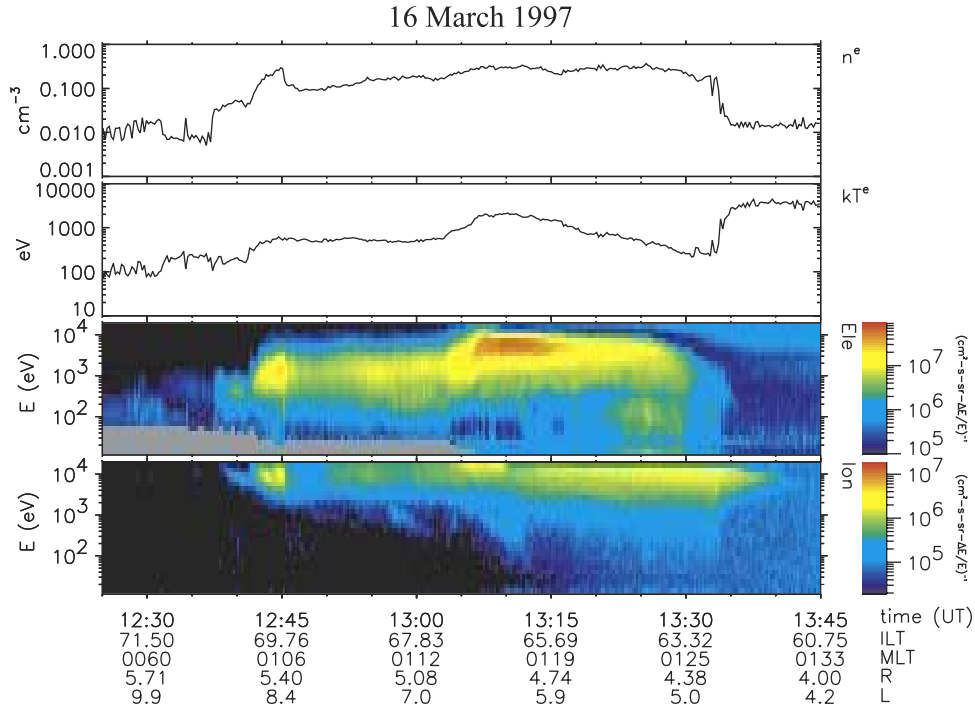

Figure 1. Electron data from a northern, high-latitude plasma sheet crossing by Polar on 16 March 1997. The top panel shows the electron density and the panel below it shows the electron mean energy. The lower two panels show omnidirectional energy-time spectrograms of electrons (just above bottom panel) and ion (bottom panel).

plasma sheet immediately adjacent to equatorward boundary and before the roll-off to zero energy.

[11] Figure 2 shows the ensemble of measurements of density and mean energy. Plotted on the right-hand side are the positions of the centers of the averages as a function of invariant latitude and MLT. As would be expected, the position information shows that the equatorward quantities are indeed at lower values of invariant latitude than the poleward values. In both cases there is variation in local time such that the lowest values of invariant latitude occur for MLT values near midnight. Note also that the poleward boundary is more variable, occasionally reaching values as high as 80° invariant latitude. The two sets of positions, taken together, roughly outline the position of the auroral oval and confirm the identification of the auroral source population as plasma sheet electrons.

[12] Plotted on the left hand side of Figure 2 is a scatterplot of density versus mean energy. Neither poleward nor equatorward sets of measurements show any significant correlation between mean energy and density. However, between the poleward and equatorward boundaries, there is a systematic variation in both parameters. Most clear is the difference in density; the poleward values cluster around 0.1 cm^{-3} and the equatorward values cluster near 0.3 cm^{-3}. There is also a difference in mean energy between poleward and equatorward measurements. The equatorward measurements show significantly more values at energies above a few hundred eV. This is consistent with the example shown in Figure 1 which showed a gradual increase in energy as Polar moved equatorward across the high-latitude plasma sheet.

[13] To understand how density and mean energy vary with respect magnetospheric location, Figures 3 and 4 show how these quantities depend on invariant latitude and MLT for poleward and equatorward cases. As before, the poleward case is shown in the top two panels and the equatorward case is shown in the bottom two panels. In both figures, the MLT variation is shown on the left-hand side and the invariant latitude variation is shown on the right-hand side. In all panels, binned medians have been overplotted with heavy lines to help elucidate the underlying trends in the data. Medians are used instead of averages to reduce the bias of points that are unusually high or low.

[14] As a function of MLT, the density data in Figure 3 show little variation. The bin medians make clear the point discussed above that the equatorward measurements have densities roughly three times that of the poleward measurements. The same trend is seen as a function of invariant latitude, particularly in the poleward measurements; as invariant latitude increases, the median density decreases.

[15] The exception is those points above 75° invariant latitude. These points appear to jump back up to densities more appropriate for the lowest latitudes. There are relatively few measurements at these high latitudes, and these points are very likely from periods of unusual conditions such as steady northward IMF B_Z and may suggest that when the poleward edge of the plasma sheet moves beyond 75° invariant latitude, the simple mapping of density to the equatorial plane becomes unreliable.

[16] The mean energy, in contrast to the density, does show variation with respect to MLT as shown in the left-hand panels of Figure 4. At the poleward edge of the high-latitude plasma sheet, there is a clear trend of significantly higher electron mean density near midnight. For the 1 hour period centered on midnight, the median mean energy is

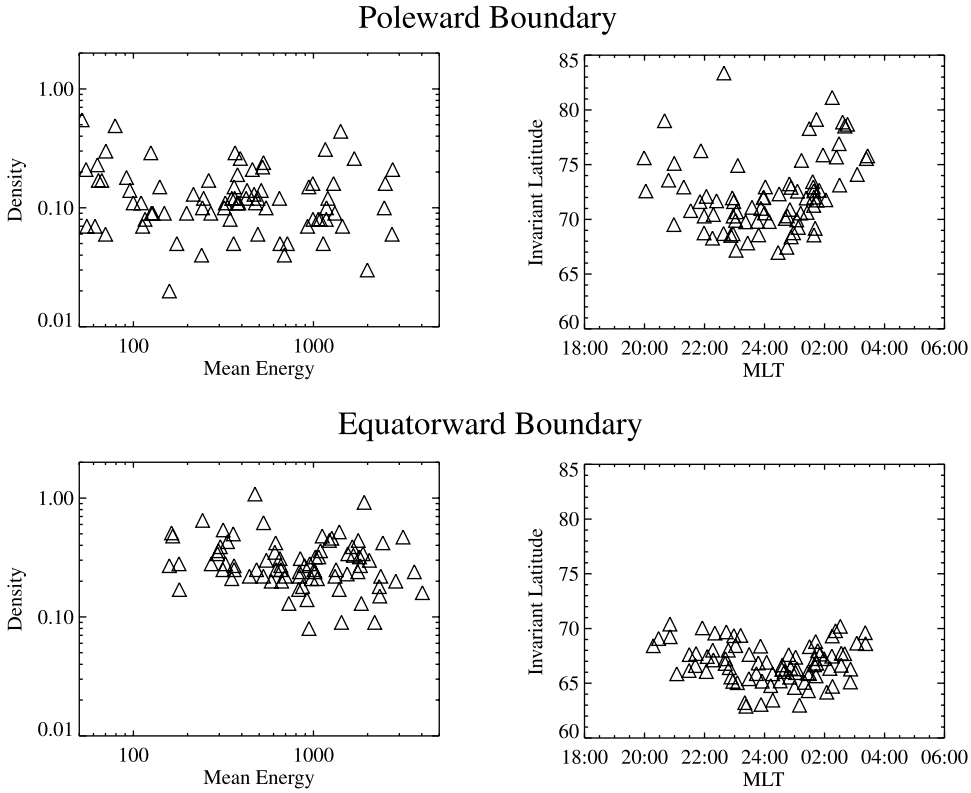

Figure 2. Fifteen minute averages of measurements of electron density and mean energy for the poleward (upper panels) and equatorward (lower panels) boundaries of the high-latitude plasma sheet. The right-hand set of panels show the positions of the averages and the left-hand panels show mean energy versus energy for each average.

1 keV which falls by an order of magnitude on either side of midnight. At the equatorward boundary of the high-latitude plasma sheet, there appears to be a gradual trend of mean energy increase from 600 to 800 eV on the eveningside to nearly 1500 eV on the morningside, although the median value closest to dawn returns the same values as for the most duskward median mean energy.

[17] As a function of invariant latitude, poleward boundary variation of the mean energy shown in the upper right panel of Figure 4 shows a decrease as latitude increases although the median values are almost constant over 67.5°–75° invariant latitude at 500–600 eV and also over 75°–80° invariant latitude at ~100 eV. At the equatorward boundary, the median value of the mean energy is essentially constant at 800–1000 eV.

4. Character of Electron Distributions

[18] In the equatorial plasma sheet the particle populations have been found to depart from the ideal Maxwellian due to the existence of a high-energy tail. *Christon et al.* [1989] analyzed the character of particle spectra from the ISEE 1 spacecraft and found that they were generally best characterized by the κ-distribution,

$$f_\kappa(v) = \frac{n}{2w^3\pi^{3/2}} \frac{\Gamma(\kappa+1)}{\kappa^{3/2}\Gamma\left(\kappa+\frac{1}{2}\right)} \left(1+\frac{v^2}{\kappa w^2}\right)^{-(\kappa+1)} \quad (1)$$

where w is the most probable speed. The advantages of the κ-distribution are that it is analytically tractable and that it adds one more parameter, κ, which affects the shape of the distribution by adding a high-energy tail. A further advantage of the κ-distribution is that in the limit $\kappa \to \infty$, the κ-distribution smoothly becomes a Maxwellian distribution:

$$f(v) = n\left(\frac{m}{2\pi k_B T}\right)^{3/2} \exp\left(-\frac{mv^2}{2k_B T}\right) \quad (2)$$

For both distributions the density n is the number of particles per unit spatial volume and can be obtained as the zeroeth moment over velocity space of the distribution. Using $kT = 2\bar{E}/3$, the relation between the temperature and the most probable speed w is

$$k_B T = \left(\frac{\kappa}{\kappa-\frac{3}{2}}\right)\frac{mw^2}{2}. \quad (3)$$

In the limit $\kappa \to \infty$, this becomes the usual relationship between temperature and most probable speed. For further details on the character of the distribution as κ changes, we refer the reader to *Dors and Kletzing* [1999].

[19] To characterize the Hydra measurements, we have performed a χ^2 fitting procedure to find best fit Maxwellian and κ-distributions for the plasma sheet crossings data set discussed above. Because the fitting procedure works with

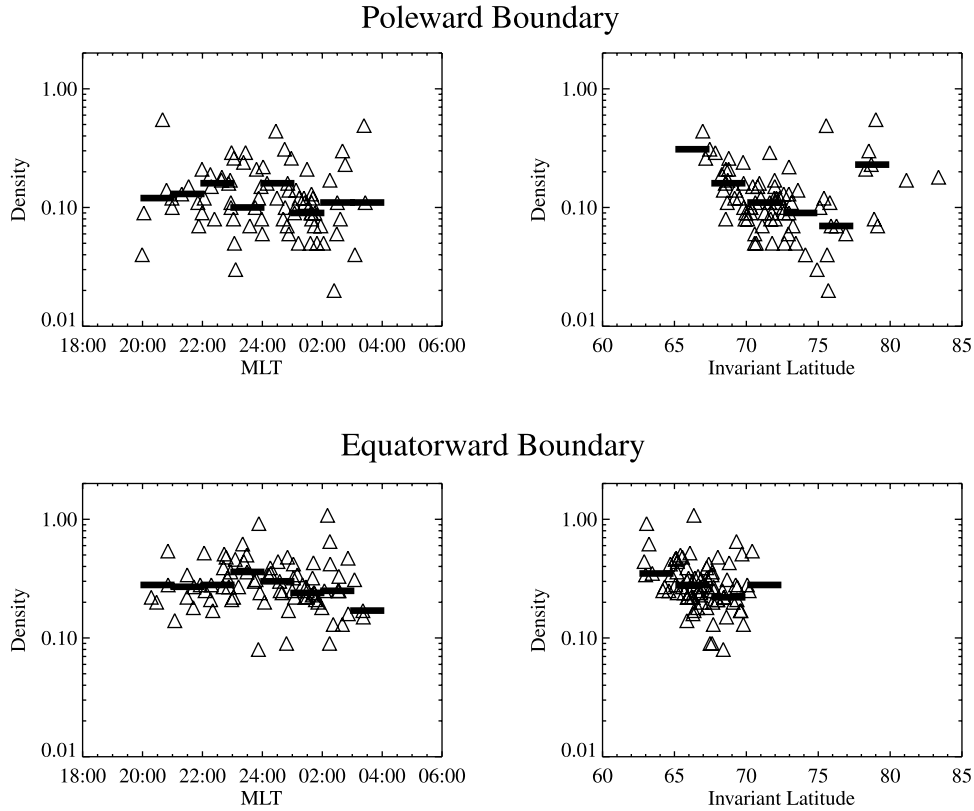

Figure 3. Variation of electron density in the high-latitude plasma sheet as a function of position. The upper panels show data from the poleward edge and the lower panels show data from the equatorward edge. The left-hand panels show variation as a function of MLT and the right-hand panels show variation as a function of invariant latitude. Heavy lines show binned medians of the measurements.

the data at all energies, it is not much affected by distributions in which the peak energy differential energy flux is not measured by the Hydra spectrometers. Hence we have used all 93 orbits for fitting electron distributions. These orbits contained 30,207 individual electron spectra, each of which was separately fitted with both a Maxwellian and κ-distribution. Because we are interested in the particles which are most important for magnetosphere-ionosphere coupling, we use spectra of electrons with pitch angles between 0° and 30° because these are the electrons which map to the auroral acceleration region. The spectra have also been corrected in energy to compensate for spacecraft potential before fitting the spectra to ensure that the fits correspond to the background plasma.

[20] Figure 5 shows an example of the Hydra data and the results of the fitting procedure for a plasma sheet crossing on 27 April 1997. The bottom four panels show Hydra particle data and electron moments in the same format as Figure 1. The top three panels show the values of the parameters obtained by the fitting procedure for both the Maxwellian distribution (red symbols, only density and temperature) and the κ-distribution (blue symbols). Plotted in green in the top two panels are the values of density and temperature obtained directly from integration of the particle data to allow comparison with the fitted parameters. The fourth panel from the bottom shows the values of reduced χ^2 (the average difference between the fit and the data normalized by the measurement error) for each fit in the same color code. A red line at $\chi^2 = 2$ has been added to this panel to help guide the eye. For most of the measured spectra the reduced χ^2 values for the kappa fits are less than the corresponding Maxwellian fit. The kappa fits are also more frequently below the $\chi^2 = 2$ line which also suggests the the kappa fits are often valid at times when no acceptable fit to a Maxwellian distribution can be found.

[21] Both the temperature and density determined from the fitting procedure are in general agreement with that from the direct moment computation using the data. The agreement between kappa and Maxwellian parameters is also quite good with almost identical temperatures over most of the plasma sheet crossing, but with the density found by the κ-distribution of the order of 10–20% higher than that from the Maxwellian fit. For this example, it is also noteworthy that the values of κ are almost all below 10 and the majority are below 5, indicating a significant high-energy tail.

[22] To better understand the differences in the fitting of kappa and Maxwellian distributions, it is useful to examine examples of the fits to individual spectra. Figure 6 shows an example of the best fit Maxwellian and κ-distributions from 27 April 1997 from 1006:21 to 1006:34. This time interval includes six sweeps of the Hydra analyzer which provides good coverage in pitch angle and good counting statistics. For each point in the spectrum, a vertical line through the point indicates the error in phase space density. As can be seen, only the points at higher energies with very small phase densities show significant error. The red curve is the

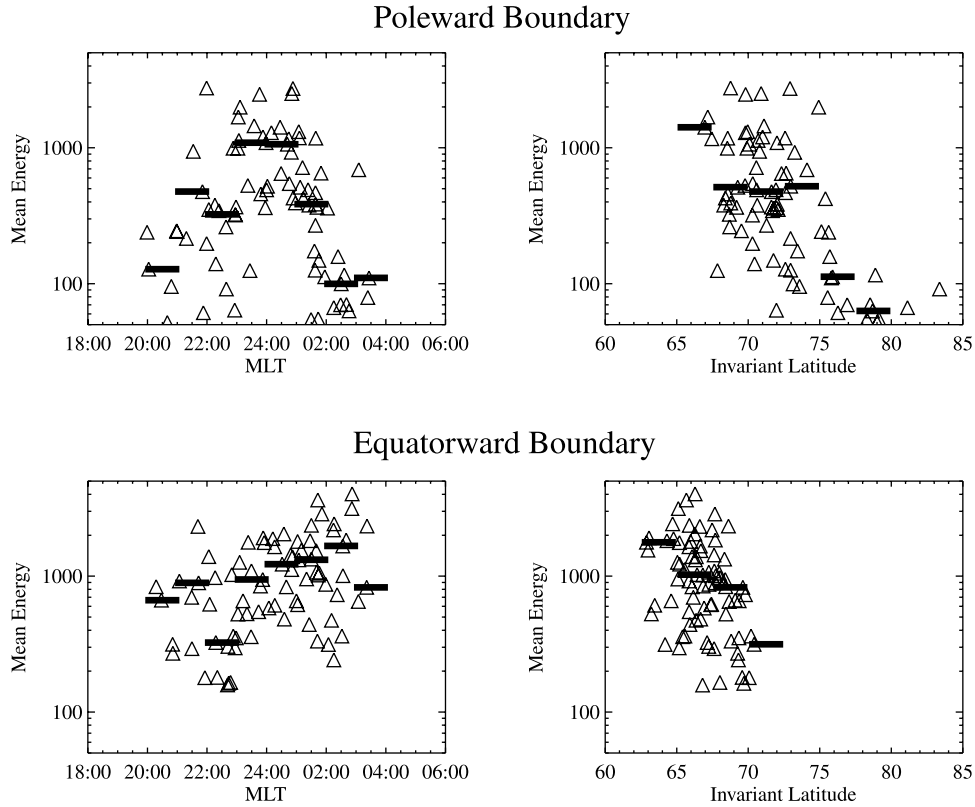

Figure 4. Variation of electron mean energy in the high-latitude plasma sheet as a function of position. The upper panels show data from the poleward edge and the lower panels show data from the equatorward edge. The left-hand panels show variation as a function of MLT and the right-hand panels show variation as a function of invariant latitude. Heavy lines show binned medians of the measurements.

best fit Maxwellian and the blue curve is the best fit κ-distribution. It is clear that the kappa distribution produces a superior fit, particularly at higher energy where the presence of a non-Maxwellian tail is apparent. The reduced χ^2 is 3.10 for the Maxwellian and 1.19 for the kappa curve. For the Maxwellian the fit lies outside the 99% confidence interval, but the κ-distribution lies well within it. For the Maxwellian distribution the fit yields a density of 0.12 cm^{-3} and temperature of 121.5 eV. For the κ-distribution the fit yields a density of 0.13 ± 0.02 cm^{-3}, temperature of 149 ± 19 eV, and a kappa value of 3.9 ± 0.6. The low value of kappa indicates significant departure from Maxwellian behavior with a power law, high-energy tail. Errors are only given for the kappa distribution because in order to find the error associated with goodness-of-fit (the majority contribution to the error), the reduced χ^2 must lie within the confidence interval of interest, 99% in this case. The Maxwellian does not meet this criterion, making consideration of errors on the fit parameters meaningless.

[23] To quantitatively compare the overall success of fitting the two types of distributions, we selected the 99% confidence intervals as the criterion for a successful fit. Out of the total 30,297 spectra which were fitted, 24% were successfully fitted with a Maxwellian distribution and 45% were successfully fitted with a κ-distribution. The success statistics may be further broken down into premidnight and postmidnight sectors. In the premidnight sector, the Maxwellian fit was successful 32.5% of the time while the kappa distribution was successful 50%. In the postmidnight sector, the success rate dropped to 20% for Maxwellian distributions and 43% for κ-distributions.

[24] In all cases, the κ-distribution is successful roughly twice as often as the Maxwellian. This suggests that the κ-distribution is a generally better description for high-latitude plasma sheet electrons than a Maxwellian distribution. This is further borne out by the fact that most of the good kappa fits have $\kappa \leq 10$ implying a significant high energy tail.

5. Correlation With Solar Wind

[25] Control of the magnetospheric response to external forcing has long been an area of study in magnetospheric physics. In particular, the role of the solar wind on plasma sheet parameters has been recently addressed by *Terasawa et al.* [1997] and *Borovsky et al.* [1998]. These reports suggest that correlations between plasma sheet and solar wind parameters exist but are best correlated when a time lag is included. To provide additional insight into these results, a comparison of solar wind parameters and high-latitude plasma sheet density and temperature as measured by Polar was undertaken. Several proposals have been made in the literature about individual and combinations of solar wind quantities which may parameterize the solar wind-magnetosphere interaction as predictors of magnetospheric activity. Because the degree of success of these parameters in predicting effects on the high latitude plasma sheet

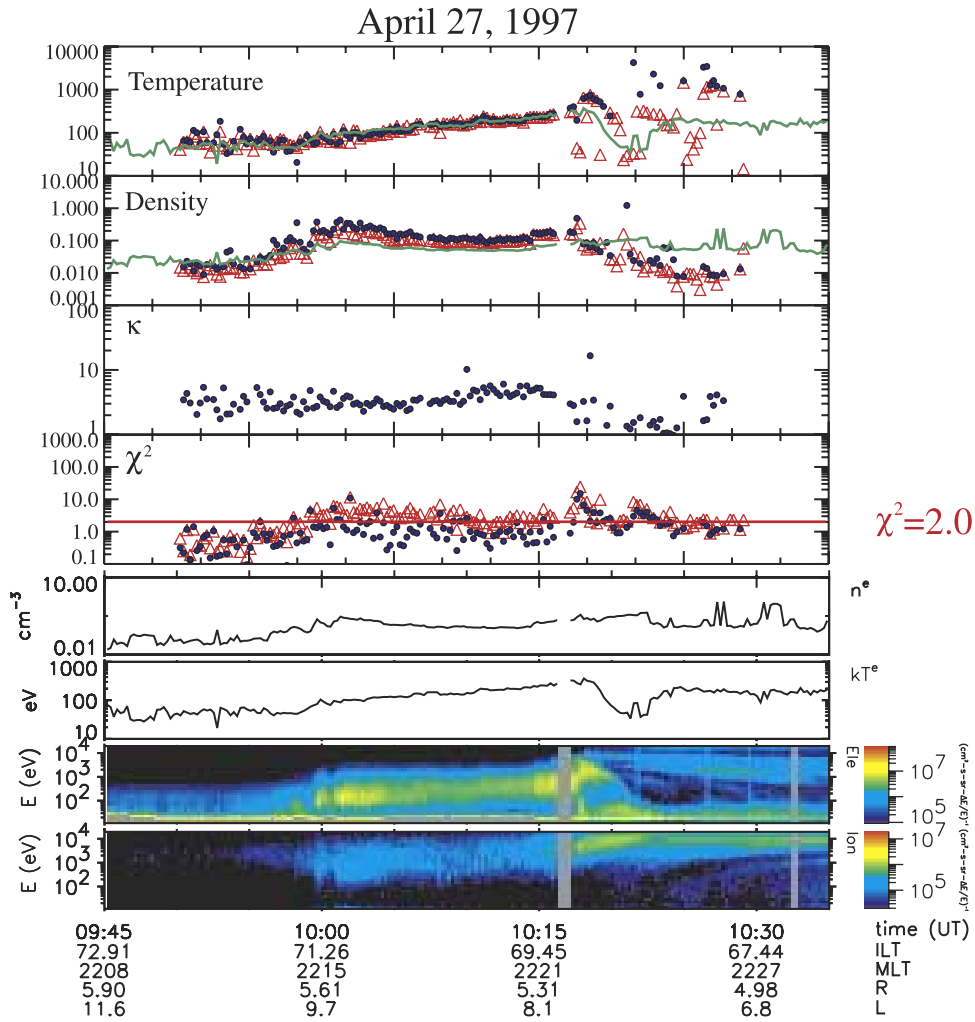

Figure 5. Comparison of Maxwellian and κ-distribution fits to Hydra electron during a plasma sheet crossing on 27 April 1997. The top three panels show the values of the fit parameters with blue symbols for the κ-distribution and red symbols for the Maxwellian distribution. The fourth panel from the top shows the value of reduced χ^2 using the same color code. The bottom four panels show particle spectrograms and electron density and temperature.

moments is not known, we made comparisons with eight parameters to ensure that we have considered a broad range of possibilities. These parameters are described in Table 1.

[26] The methodology for comparison was to take the same 15 min averages of high-latitude plasma sheet density and temperature discussed above and to compare them with 1 hour averages of the eight solar wind parameters as measured on the Wind satellite. For each of the solar wind parameters, 1 hour averages were constructed for the preceding 18 hours from the time of the plasma sheet measurements. Before constructing the 1 hour averages, the solar wind data were adjusted in time to account for the propagation from Wind to the Earth by using the upstream distance of the spacecraft and the solar wind velocity at that time. One hour intervals for the averages were selected to extract the longer term trends in the solar wind so as to minimize the effects of transients which might skew the results.

[27] The data were then plotted as scatterplots with plasma sheet averages along the x-axis and the relevant solar wind parameter along the y-axis. As shown in Figure 7, plots were constructed for each 1 hour offset backward in time (after correction for solar wind propagation) from when the high-latitude plasma sheet averages were calculated. This example shows a comparison of poleward high-latitude plasma sheet electron density with solar wind proton density. As a measure of correlation, the linear correlation factor R was computed for each 1 hour average [*Bevington*, 1969]. The data in each panel were also fitted to a line. Two measures of best fit were computed: the usual χ^2 minimization and an absolute value deviation. Within each panel, each point represents a single high plasma sheet crossing. To give a degree of "robustness," to the calculation of R, all crossings except for the two pairs which produced the largest contributions to the calculation of χ^2 are used in the calculation of R and the linear fits. These outliers were removed to exclude the possibility of a couple of anomalous points reducing the cross correlation. The outlier removal does not significantly alter the essential results but does somewhat improve the values of R which

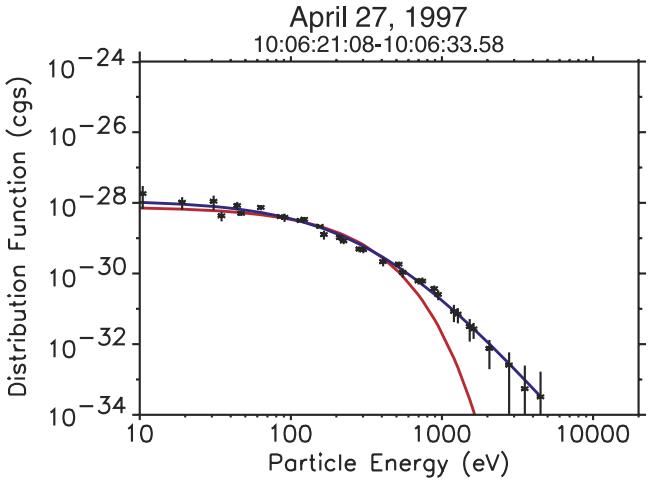

Figure 6. Example of Maxwellian (red curve) and kappa (blue curve) distribution fits to electron spectra in the high latitude plasma sheet. The kappa fit is within the 99% confidence interval, but the Maxwellian is not. The fit finds $\kappa = 3.9 \pm 0.6$. The low value of κ indicates a significant high-energy tail as is apparent in the figure.

are computed. This left 78 pairs of measurements for each plot.

[28] The results of the comparisons in Figure 7 are shown in Figure 8. The upper panels shows the linear cross-correlation coefficient R. True correlation is difficult to prove, but one can test against the null hypothesis. Lines corresponding to R_{null} such that only one in 10,000 random data sets would produce a correlation above this level are plotted in the upper panel of Figure 8 to indicate significance. Values of R which lie between these two lines are indistinguishable from random variation at the 99.99% confidence level.

[29] The middle panel of Figure 8 shows reduced χ^2 as a function of time delay. For the plasma sheet data from Hydra, we include errors from counting statistics and the energy bandwidth of the detector. Because we do not have a easy way to calculate the error for each value of the solar wind parameters, we have chosen to use an error which is the greater of either 20% of the value of each point or 5% of the mean value of all the points. This latter quantity is used to provide a minimum error in order to avoid overweighting points with small values. This error estimate gives us a conservative estimate which allows us to use the reduced χ^2 to give some sense of how well a linear relationship describes the correlation between solar wind and plasma sheet parameters. For a fit to be considered good, reduced χ^2 should have a value less than 1.5; a value of near 3, such as is found here, indicates that the relationship is not strongly linear.

[30] The lower panel in Figure 8 shows the reduced absolute deviation as a function of delay time. This is calculated as the sum of the absolute values of the differences between the data values and the best fit line normalized by the mean error and the number of degrees of freedom. This avoids the quadratic dependence in the definition of χ^2 which heavily weights outliers in determining the best fit and may do a better job of fitting the bulk of the data in a situation in which there is large scatter. Both reduced χ^2 and reduced absolute deviation show minima near where the peak in R occurs. Although the correlation between solar wind density and plasma sheet density is not strongly linear, it is most like a linear relation for a time delay of about 3.5 hours.

[31] To investigate which of the solar wind parameters correlate with plasma sheet density, in Figure 9 we show the three figures of merit shown in Figure 8 for all eight of the solar wind parameters given in Table 1 for the poleward plasma sheet crossings. In examining this table, we consider only those quantities for which the correlation coefficient is greater than that expected for the null hypothesis. This eliminates ϵ and vB^2. Of the remaining quantities, we concentrate those parameters with the lowest values of reduced χ^2. Ideally, we would have values of reduced χ^2 near 1. Of the six quantities, however, two have significantly lower values with reduced $\chi^2 \leq 5$ and values of absolute deviation ≤ 3 suggesting that these correlations are relatively linear. These two parameters are the solar wind density ($n_{p,SW}$) and solar wind particle flux ($n_{p,SW}v$) which have the highest correlations with $R = 0.613$ and $R = 0.575$, respectively. In both cases, a gentle peak at 3.5 hours of delay time is found.

[32] For the best fit line, we use the reduced χ^2 as the better description because it includes the proper error weight for both solar wind and plasma sheet quantities. The solar wind density -high-latitude plasma sheet density correlation linear fit is

$$n_{PS} = 0.022 n_{SW} - 0.040 \quad (4)$$

For the relation between solar wind flux and the high-latitude plasma sheet we have

$$n_{PS} = 7.43 \times 10^{-10} \Gamma_{SW} - 0.076 \quad (5)$$

Table 1. Summary of Solar Wind Parameters Used to Correlate With High-Latitude Plasma Sheet Density and Temperature

Quantity	Physical Description	Reference
B_Z	north-south B	*Fairfield and Cahill* [1966]
vB_Z	dawn-dusk E	*Aubry and McPherron* [1971]
vB^2	magnetic energy density flux	*Baker et al.* [1981]
v^2B_z	energy input rate	*Murayama and Hakamada* [1975]
$n_{P,sw}$	solar wind proton density	*Borovsky et al.* [1997]
nv	solar wind proton flux	this paper
$nv^2B_z/2$	solar wind dynamic pressure coupling	*Song and Lysak* [1994]
ϵ	Poynting flux input	*Perreault and Akasofu* [1978]

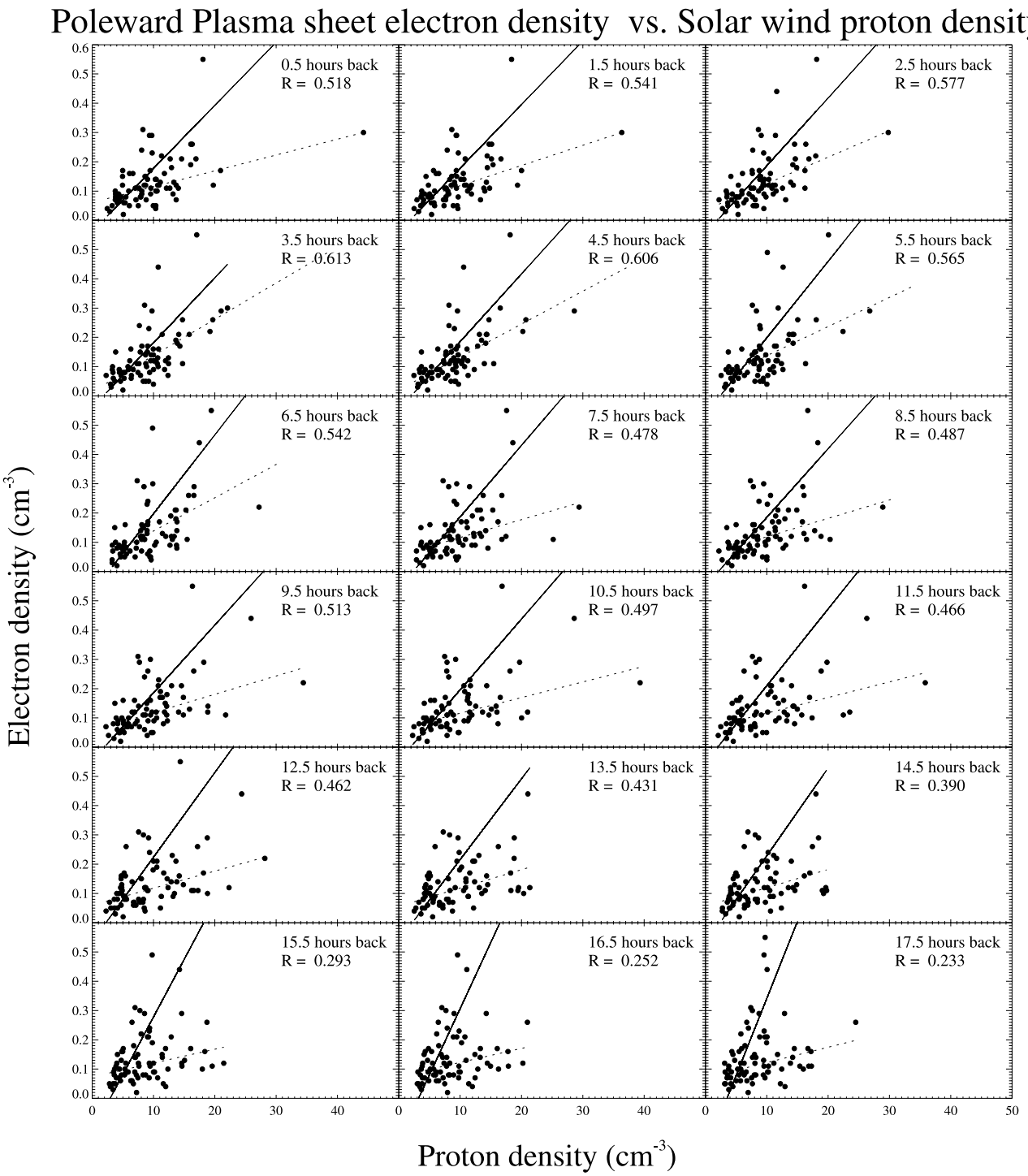

Figure 7. Example of the cross-correlation technique between 1 hour averages of solar wind parameters and 15 min averages of high-latitude plasma sheet density and temperature. The example shown is for a comparison of solar wind proton density and poleward high-latitude plasma sheet electron density. Each panel shows the two quantities plotted as a scatterplot for a series of offsets in the solar wind averages backwards in time from when the plasma sheet data were measured. Lines are shown for the best χ^2 (solid) and absolute value (dashed) fits to the data.

where Γ_{SW} is the solar wind flux in cm^{-2}-s^{-1}. Note that in both cases, small values of solar wind density and flux can give negative values which have no meaning.

[33] The solar wind parameters were also checked for correlation with the mean energy of the poleward high-latitude electrons. For all eight solar wind parameters, no correlation value greater than the null result were found, suggesting that mean energy in this region does not correlate with the solar wind.

[34] In Figure 10, the same correlation measures shown in Figure 9 are shown for crossings on the equatorward side of the high-latitude plasma sheet. For this case, four of the solar

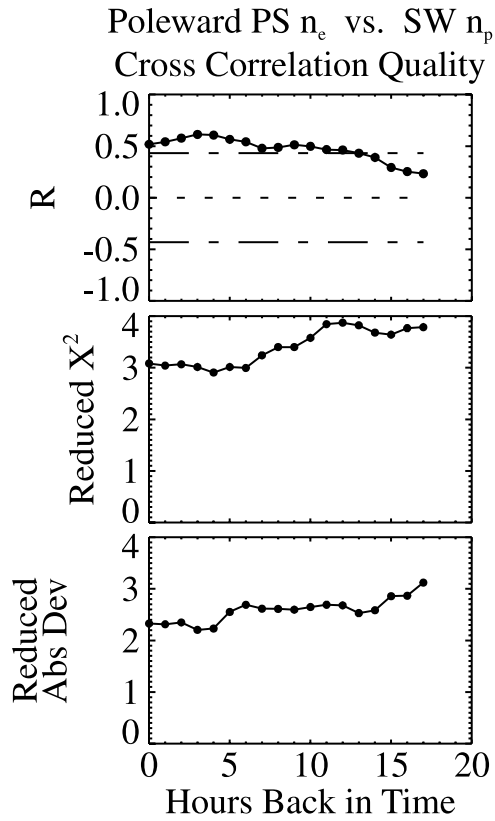

Figure 8. Cross-correlation figures of merit as a function of hours of delay of the solar wind parameters in Figure 7. The upper panel shows R, the middle panel shows the best linear fit reduced χ^2, and the bottom panel shows the best linear fit using reduced absolute value deviation.

wind parameters show correlation above the threshold for null result: ϵ, solar wind particle flux, solar wind density, and vB^2. Of these, ϵ and vB^2 have the lowest correlations with $R = 0.556$ and $R = 0.591$, respectively. Both solar wind density and flux have significantly higher correlations with $R = 0.694$ and $R = 0.725$, respectively. Applying the linearity criteria, that is, reduced $\chi^2 \leq 5$ and low values of absolute deviation at the point of maximum R, further suggests that solar wind particle flux and solar wind density have the best correlations, although vB^2 does does marginally better than ϵ. For both the solar wind particle flux and the solar wind density, the peak correlation occurs for a time delay of 3.5 hours. This suggests that both the solar wind particle flux and density are moderately good predictors of high-latitude plasma sheet density nearest the equatorial boundary.

[35] For the best fit line, the reduced χ^2 fit for the solar wind flux - high latitude plasma sheet density correlation linear fit is

$$n_{PS} = 1.54 \times 10^{-9}\Gamma_{SW} - 0.11 \quad (6)$$

where Γ_{SW} is the solar wind flux in cm^{-2}-s^{-1}. For the relation between solar wind flux and the high-latitude plasma sheet we have

$$n_{PS} = 0.050 n_{SW} - 0.51 \quad (7)$$

As before, small values of solar wind density and flux can give negative values which have no meaning.

[36] We also looked for correlation with equatorward electron mean energy with the solar wind parameters. These results are shown in Figure 11. Four quantities show correlation above the null result threshold but in all cases with with $|R| < 0.55$. These four quantities were B_Z, dawn-dusk electric field, v^2B_Z, and $nv^2B_Z/2$. All but the dawn-dusk electric field showed negative correlation. The strongest negative correlation is for v^2B_Z with $R = -0.540$. Close to this were B_Z and dawn-dusk electric field with $R = -0.523$ and $R = 0.525$, respectively. The ϵ parameter is so marginally above null hypothesis threshold that it can be neglected. The negative correlations mean that the equatorward high-latitude plasma sheet electron mean energy decreased for increasing values of the solar wind parameter. All of the correlated parameters have dependence on solar wind B_Z (the dawn dusk electric field is defined as vB_Z), suggesting decreasing energy for northward IMF. The three correlated parameters showed very poor linearity in all cases as characterized by reduced $\chi > 15$ and absolute deviation between 4 and 5. Consequently, the best fit line fits are of low reliability and will not be presented. The mild correlations suggest a weak coupling of the IMF B_Z component to the mean energy of high-latitude plasma sheet electrons.

6. Summary of Results

[37] In summary, we have found the following average properties of the electron population of the nightside high-latitude plasma sheet during Polar transits through this region at radial distances of 4–7 R_E during the time period of February–May, 1997:

[38] 1. The median electron density of the high-latitude plasma sheet ranges from 0.1 cm^{-3} on the poleward boundary to 0.3 cm^{-3} on the equatorward boundary. The average electron mean energy ranges from 400 eV on the poleward boundary to 900 eV on the equatorward boundary.

[39] 2. The character of the electron spectrum of the high-latitude plasma sheet is best described by the κ distribution with values of $\kappa \leq 10$. Overall the κ distribution is twice as successful as the Maxwellian distribution in providing a statistically acceptable fit to the data.

[40] 3. The solar wind quantities which best correlate with high-latitude plasma sheet electron density are the solar wind density and the solar wind particle flux with a delay time of 3–4 hours. The correlation is strongest for the equatorial side of the high-latitude plasma sheet but holds for both sides. The mean energy of the high-latitude plasma sheet electrons shows a weak inverse correlation with quantities associated the orientation of the solar wind B_Z component of the magnetic field and delay of 1–2 hours. However, this correlation is not very linear, suggesting that this connection may be complex.

7. Discussion

[41] The values of the electron mean energy and density calculated from the Hydra measurements of the high-latitude plasma sheet are in good agreement with those found by several studies of equatorial plasma sheet plasma parameters [*Slavin et al.*, 1985; *Baumjohann et al.*, 1988]. Hydra

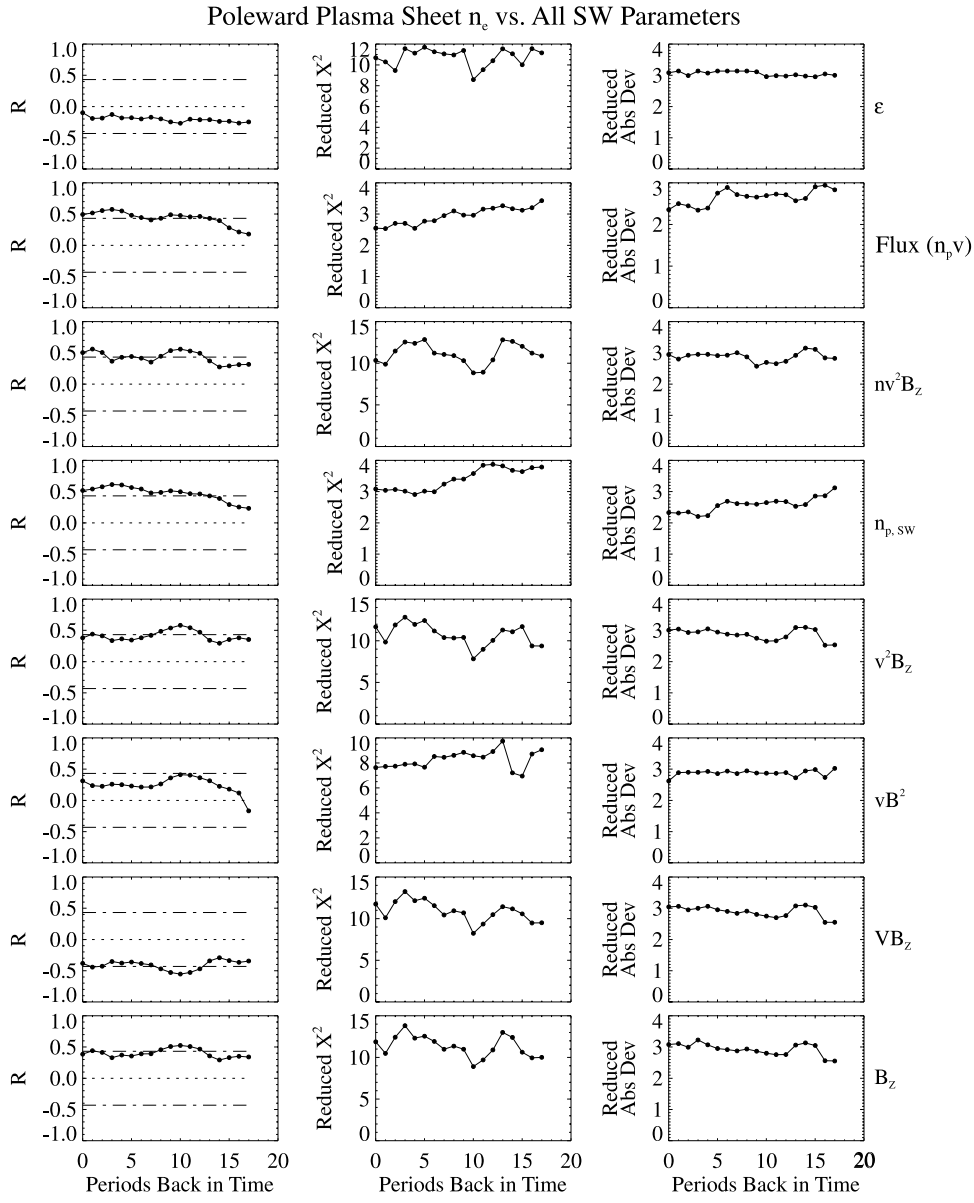

Figure 9. Comparison of poleward plasma sheet density with eight different solar wind parameters as a function of delay time. Three different figures of merit are shown. The left column shows the linear correlation coefficient R, the middle column shows the reduced χ^2 of the best fit line, and the right column shows the reduced absolute deviation.

data has established that these high-latitude plasma sheet electrons show distribution functions which are consistent with a connection to auroral ionosphere below the spacecraft [*Kletzing and Scudder*, 1999]. This provides a confirmation that the equatorial plasma sheet provides the electrons which are the source population for the aurora.

[42] The increase in density from the poleward to equatorward side of the high-latitude plasma sheet mirror similar observations of plasma density in the equatorial plasma sheet which showed the lowest density at the plasma sheet boundary layer and higher density in the central plasma sheet [*Baumjohann et al.*, 1988]. The decrease in density with increasing latitude is an expression of the local equatorial plasma sheet density to which these points map. As latitude increases, the high-latitude plasma sheet maps to regions which increase in distance down the magnetotail. As one moves down the tail, the background plasma density decreases as the magnetic field drops so as to maintain pressure balance. The mapping of the equatorial points of highest density corresponds to points closest to the Earth and smallest values of invariant latitude, exactly the trend seen here.

[43] The connection of the poleward boundary of the high-latitude plasma sheet electrons to the more distant is also suggested by the distribution of density measurements about the median value. The poleward measurements have a spread of values over 0.01–0.1 cm^{-3}. The same type of spread in density values has also been found in studies of the more distant magnetotail which also show substantial skew from an average density of 0.1 cm^{-3} towards values

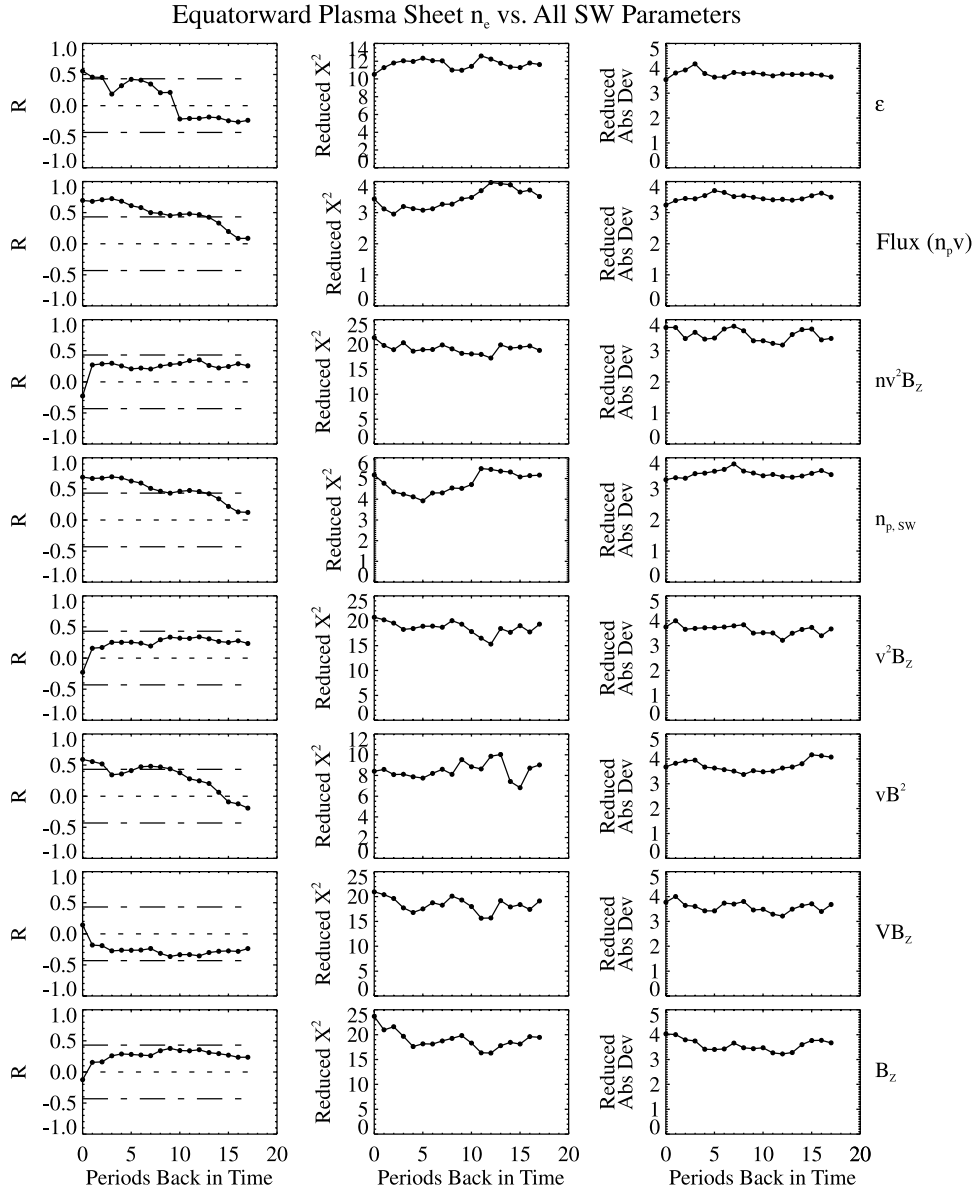

Figure 10. Comparison of equatorward plasma sheet density with eight different solar wind parameters as a function of delay time. Three different figures of merit are shown. The left column shows the linear correlation coefficient R, the middle column shows the reduced χ^2 of the best fit line, and the right column shows the reduced absolute deviation.

below 0.1 cm^{-3} for observations at distances beyond 60 R_E [*Zwickl et al.*, 1984].

[44] There is only weak evidence in the Polar observations of the high-latitude plasma sheet for a "superdense" plasma sheet (density of 2–5 cm^{-3}) as reported by *Borovsky et al.* [1997]. The clearest evidence of the superdense plasma sheet came from geosynchronous observations. This would most closely correspond to the equatorward Polar measurements. Indeed, the two largest density measurements are from the equatorward observations with values slightly less than 1.0 cm^{-3}. Both of these highest density measurements occur near sudden increases of the K_p index as was also reported for the superdense geosynchronous spacecraft measurements [*Borovsky et al.*, 1997]. Several such K_p increases occurred (3–5 per month) during the interval for the study reported here. However, *Borovsky et al.* [1998] indicated a 6% occurrence rate for the superdense plasma sheet which would predict five such events in a data set of 78 measurements. We do not see this many. The geosynchronous measurements also had an average density more than twice the largest values observed by Polar. This suggests that the superdense enhancement is greatest near geosynchronous orbit and is not representative of the plasma sheet as a whole. This is consistent with a plasmaspheric source of enhanced density as suggested by *Borovsky et al.* [1997].

[45] The trend of increasing electron mean energy from poleward to equatorward boundary of the high-latitude plasma sheet has also been observed in the equatorial plasma sheet. Equatorial observations of ion temperature

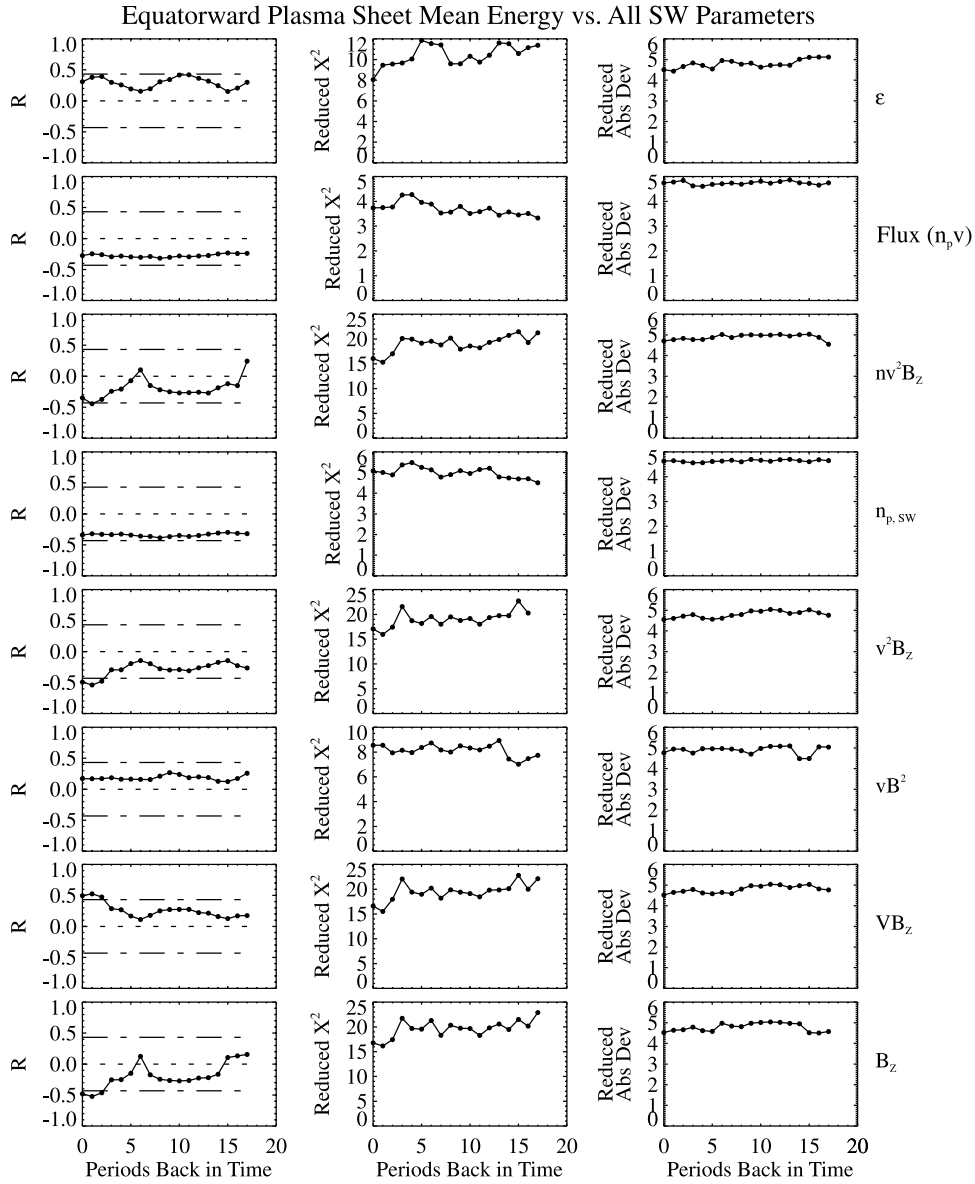

Figure 11. Comparison of equatorward plasma sheet mean energy with eight different solar wind parameters as a function of delay time. Three different figures of merit are shown. The left column shows the linear correlation coefficient R, the middle column shows the reduced χ^2 of the best fit line, and the right column shows the reduced absolute deviation.

made by AMPTE/IRM between 9 and 19 R_E tailward show a clear trend of increasing energy as one moves from the plasma sheet boundary layer to the central plasma sheet [*Baumjohann et al.*, 1988]. This trend is also seen in equatorial plasma sheet electron measurements which show a clear decrease in electron temperature with radial distance from the Earth in the tailward direction [*Zwickl et al.*, 1984].

[46] The increase in average energy near midnight observed at the poleward high-latitude plasma sheet stands out in the data. These observations cannot be those of directly accelerated upgoing electrons, since the upward accelerated electrons map to very small pieces of the overall electron phase space at these altitudes and contribute little to the mean energy; the mean energy is dominated by the background electrons. It is most likely that this increase in mean energy is associated with equatorial plasma sheet energy buildup such as the plasma injections observed by geosynchronous spacecraft [*DeForest and McIlwain*, 1971].

[47] The finding that the character of the high-latitude plasma sheet electrons is best described by a κ distribution is again consistent with equatorial plasma sheet observations. ISEE 1 measurements of both electrons and ions have shown that κ distributions provide the best description of the equatorial distribution over a wide range of energies and for geomagnetically quiet conditions [*Christon et al.*, 1989]. Theoretical efforts have shown that the transport of mantle and lobe plasma into the plasma sheet results in κ distributions [*Schriver et al.*, 1998]. Lobe plasma has been identified with the strahl component of the solar wind [*Fairfield and Scudder*, 1985] and solar wind electrons have been

shown to be fit by κ distributions [*Maksimovic et al.*, 1998]. The lobe plasma may already have κ character before it is transported to the plasma sheet. Given the connection that has been reported of these high-latitude plasma sheet electrons to the auroral ionosphere [*Kletzing and Scudder*, 1999], this suggests that models of the auroral acceleration region should include the effects of κ distributions. One simple model, based on the *Knight* [1973] relation between auroral current and potential drop, has shown that κ distributions should have noticeable effects, producing different acceleration profiles than those expected for Maxwellian distributions [*Dors and Kletzing*, 1999].

[48] The correlation of solar wind with high-latitude plasma sheet parameters is strongest for the correlation between solar wind density and flux and plasma sheet density. This result is consistent with prior comparisons of solar wind density with that of the plasma sheet [*Terasawa et al.*, 1997; *Borovsky et al.*, 1997, 1998]. In these studies it was also found that there is a time lag associated with the time of best correlation of the plasma sheet data with the solar wind density. *Borovsky et al.* [1998] found the best correlation with data at 17–22 R_E occurred for a 1–4 hour delay. We also find similar delays for best correlation. The results from *Terasawa et al.* [1997] show the best correlation for an average of the solar wind density over the 9 hours preceding the measurement in the equatorial plasma sheet. For an average, one usually associates the center of the period over which the average takes place with the time for the average value. This would yield a delay time of 4.5 hours, which is consistent with the Polar measurements reported here.

[49] These results suggest that the solar wind is the dominant source of particles for the plasma sheet, consistent with transport of solar wind plasma across the magnetosheath to the mantle. As discussed by *Pilipp and Morfill* [1978], the particle supply from the mantle is sufficient to replenish losses from the plasma sheet. This model has been made more concrete in recent work by *Schriver et al.* [1998] which showed that mantle and lobe sources of electrons and ions will be heated and transported to the plasma sheet yielding the appropriate temperatures and temperature ratio between electrons and ions. Although they do not directly discuss the point, the figures in this report suggest that transport times from the mantle to the plasma sheet are of the order of 1–4 hours as discussed above.

[50] The correlations of the solar wind with with high-latitude plasma sheet electron mean energy are not as clear as those for density. For the poleward measurements, there is no significant correlation. However, the equatorial side does show correlation, although not at particularly high levels. In all cases, the solar wind parameters which correlate have a dependence on the B_Z component of the IMF. The character of this relation is an anticorrelation; when the IMF is northward (positive), the mean energy of the plasma sheet electrons decreases and when it is southward (negative), the mean energy increases. This anticorrelation peaks at 1 hour of delay, indicating that the magnetospheric response is relatively quick in the heating of plasma sheet electrons. The anticorrelation of IMF B_Z with plasma sheet mean energy is consistent with the results of *Terasawa et al.* [1997], who found the that temperature of the equatorial plasma sheet decreased for northward IMF conditions. They found the best anticorrelation for a 5 hour average of the IMF B_Z component preceding the measurement in the plasma sheet. Following our earlier reasoning, this 5 hour average would center on a delay time of 2.5 hours, consistent with our results.

[51] Such an anticorrelation with IMF B_Z is not surprising because the IMF B_Z component is widely thought to be critical to the rate of magnetic reconnection at the dayside magnetopause. Under southward IMF conditions, merging is most favored and allows the greatest energy input into the magnetospheric system. Under northward IMF conditions, the merging rate is reduced and less energy input results.

8. Conclusions

[52] Observations of the electrons in the high-latitude plasma sheet observed by Polar make clear that there is a great degree of similarity in basic structure with that found in the equatorial plasma sheet. This includes average values of density and temperature as well as the κ-distribution character of the distribution function. When coupled with prior, detailed observations of the electron distributions in this region which show that this region is connected to the Earth's auroral region at the ionospheric end of the field line, it is clear that the plasma sheet is the source of the electrons which are accelerated in auroral processes.

[53] This study also makes clear that there is a connection between the solar wind and the plasma sheet which carries over to its high-latitude extension. Solar wind density shows good correlation with high-latitude plasma sheet electron density, very similar to the correlation between plasma sheet density and solar wind density and with similar time delays of 1–4 hours for propagation of material through the magnetospheric system. There is also a weaker connection between IMF B_Z and high-latitude plasma sheet electron mean energy as is seen in equatorial plasma sheet data.

[54] The new data presented here on these basic parameters of the high-latitude plasma sheet electron population will allow auroral modelers to more accurately determine input conditions for building models of the auroral acceleration process. Moreover, with the understanding of some of the dependencies on solar wind parameters, models which seek to match specific examples of auroral data can be guided by the input parameters which are most appropriate for the comparison based on solar wind monitoring.

[55] **Acknowledgments.** This work performed under NASA grant NAG5-2231 and DARA grant 50-OC-89110. The results of the HYDRA investigation were made possible by the decade-long hardware efforts of groups led at NASA GSFC by K. Ogilvie, at UNH by R. Torbert, at MPAe by A. Korth, and at UCSD by W. Fillius. The authors would also like to acknowledge the use of solar wind magnetic field data from the WIND MFI experiment (R. Lepping, PI) and solar wind plasma data from the WIND SWE experiment (K. Ogilvie, PI) which are both part of the NASA/GSFC Laboratory for Extraterrestrial Physics.

[56] Arthur Richmond thanks Charles W. Carlson and Patrick T. Newell for their assistance in evaluating this paper.

References

Aubry, M. P., and R. L. McPherron, Magnetotail changes in relation to the solar wind magnetic field and magnetospheric substorms, *J. Geophys. Res.*, *76*, 4381, 1971.

Baker, D. N., J. E. W. Hones, J. B. Payne, and W. C. Feldman, A high time resolution study of interplanetary parameter correlations with AE, *Geophys. Res. Lett.*, *8*, 179, 1981.

Baumjohann, W., G. Paschmann, N. Sckopke, C. A. Cattell, and C. W. Carlson, Average ion moments in the plasma sheeet boundary layer, *J. Geophys. Res.*, *93*, 11,507, 1988.

Baumjohann, W., G. Paschmann, and C. A. Cattell, Average plasma properties in the central plasma sheeet, *J. Geophys. Res.*, *94*, 6597, 1989.

Bevington, P. R., *Data Reduction and Error Analysis for the Physical Sciences*, McGraw-Hill, New York, 1969.

Borovsky, J. E., M. F. Thompson, and D. J. McComas, The superdense plasma sheet: Plasmasphere origin, solar wind origin, or ionospheric origin?, *J. Geophys. Res.*, *102*, 22,089, 1997.

Borovsky, J. E., M. F. Thompson, and R. C. Elphic, The driving of the plasma sheet by the solar wind, *J. Geophys. Res.*, *103*, 17,617, 1998.

Christon, S. P., D. G. Mitchell, D. J. Williams, L. A. Frank, C. Y. Huang, and T. E. Eastman, Energy spectra of plasma sheet ions and electrons from ∼50 ev/e to ∼1 mev during plasma temperature transitions, *J. Geophys. Res.*, *93*, 2562, 1988.

Christon, S. P., D. J. Williams, D. G. Mitchell, L. A. Frank, and C. Y. Huang, Spectral characteristics of plasma sheet ion and electron populations during undisturbed geomegnetic conditions, *J. Geophys. Res.*, *94*, 13,409, 1989.

DeForest, S. E., and C. E. McIlwain, Plasma clouds in the magnetosphere, *J. Geophys. Res.*, *76*, 3587, 1971.

Dors, E. E., and C. A. Kletzing, Effects of suprathermal tails on auroral electrodynamics, *J. Geophys. Res.*, *104*, 6783, 1999.

Fairfield, D. T., and L. J. Cahill Jr., Transition region magnetic field and polar magnetic disturbances, *J. Geophys. Res.*, *71*, 155, 1966.

Fairfield, D. T., and J. D. Scudder, Polar rain: Solar coronal electrons in the Earth's magetosphere, *J. Geophys. Res.*, *90*, 4055, 1985.

Frank, L. A., W. R. Patterson, K. L. Ackerson, S. Kokubun, and T. Yamamoto, Plasma velocity distributions in the near-Earth plasma sheet: A first look with the Geotail spacecraft, *J. Geophys. Res.*, *101*, 10,627, 1996.

Huang, C. Y., and L. A. Frank, A statistical study of the central plasma sheet: Implications for substorm models, *Geophys. Res. Lett.*, *13*, 652, 1986.

Huang, C. Y., and L. A. Frank, A statistical survey of the central plasma sheet, *J. Geophys. Res.*, *99*, 83, 1994.

Kistler, L. M., W. Baumjohann, T. Nagai, and E. Mobius, Superposed epoch analysis of pressure and magnetic field configuration changes in the plasma sheet, *J. Geophys. Res.*, *98*, 9249, 1993.

Kletzing, C. A., and J. D. Scudder, Auroral-plasma sheet electron anisotropy, *Geophys. Res. Lett.*, *26*, 971, 1999.

Knight, L., Parallel electric fields, *Planet. Space Sci.*, *21*, 4326, 1973.

Maksimovic, M., V. Pierrard, and P. Riley, Ulysses electron distributions fitted with Kappa functions, *Geophys. Res. Lett.*, *24*, 1151, 1998.

Murayama, T., and K. Hakamada, Effects of solar wind parameters on the development of magnetospheric substorms, *Planet. Space Sci.*, *23*, 75, 1975.

Newell, P. T., Y. I. Feldstein, Y. I. Galperin, and C. I. Meng, Morphology of nightside precipitation, *J. Geophys. Res.*, *101*, 10,737, 1996.

Perreault, P., and S.-I. Akasofu, A study of geomagnetic storms, *Geophys. J. R. Astron. Soc.*, *54*, 547, 1978.

Pilipp, W. G., and G. Morfill, The formation of the plasma sheet resulting from plasma mantle dynamics, *J. Geophys. Res.*, *83*, 5670, 1978.

Schriver, D., M. Ashour-Abdala, and R. L. Richard, On the origin of the ion-electron temperature difference in the plasma sheet, *J. Geophys. Res.*, *103*, 14,879, 1998.

Scudder, J., et al., Hydra—A 3-dimensional electron and ion hot plasma instrument for the Polar spacecraft of the GGS mission, *Space Sci. Rev.*, *71*, 459, 1995.

Slavin, J. A., E. J. Smith, D. G. Sibeck, D. N. Baker, R. D. Zwickl, and S.-I. Akasofu, An ISEE 3 study of average and substorm conditions in the distant magnetotail, *J. Geophys. Res.*, *90*, 10,875, 1985.

Song, Y., and R. L. Lysak, Alfvénon driven reconnection and the direct generation of field-aligned current, *Geophys. Res. Lett.*, *21*, 1755, 1994.

Spence, H. E., M. G. Kivelson, R. J. Walker, and D. J. McComas, Magnetospheric plasma pressures in the midnight meridian: Observations from 2.5 to 34 R_E, *J. Geophys. Res.*, *94*, 5264, 1989.

Terasawa, T., et al., Solar wind control of density and temperature in the near-earth plasma sheet: WIND/GEOTAIL collaboration, *Geophys. Res. Lett.*, *24*, 935, 1997.

Wing, S., and P. T. Newell, Central plasma sheet ion properties as inferred from ionospheric observations, *J. Geophys. Res.*, *103*, 6785, 1998.

Zwickl, R. D., D. N. Baker, S. J. Bame, W. C. Feldman, J. T. Gosling, E. W. Hones Jr., and D. J. McComas, Evolution of the Earth's distant magnetotail: ISEE 3 electron plasma results, *J. Geophys. Res.*, *89*, 11,007, 1984.

C. Curto, Department of Mathematics, Duke University, Box 90320, Durham, NC 27708-0320, USA. (ccurto@math.duke.edu)

E. E. Dors, Los Alamos National Laboratory, P. O. Box 1663, MS D466, Los Alamos, NM 87545, USA. (edors@lanl.gov)

C. A. Kletzing and J. D. Scudder, Department of Physics and Astronomy, University of Iowa, 203 Van Allen Hall, Iowa City, IA 52242, USA. (craig-kletzing@uiowa.edu; jds@space-theory.physics.uiowa.edu)